

Meson-Nucleon Scattering Amplitudes from Lattice QCD

John Bulava^{a)}

CP3-Origins, University of Southern Denmark, Campusvej 55, 5230 Odense M, Denmark

^{a)}*Electronic mail: bulava@cp3.sdu.dk*

Abstract. Lattice QCD calculations of resonant meson-meson scattering amplitudes have improved significantly due to algorithmic and computational advances. However, progress in meson-nucleon scattering has been slower due to difficulties in computing the necessary correlation functions, the exponential signal-to-noise problem, and the finite-volume treatment of scattering with fermions. Nonetheless, first benchmark calculations have now been performed. The status of lattice QCD calculations of meson-nucleon scattering amplitudes is reviewed together with comments on future prospects.

Meson-nucleon scattering amplitudes are required in a variety of active research areas of nuclear and particle physics. Near threshold they provide valuable determinations of the low-energy constants (LEC's) of chiral perturbation theory involving baryons, which also govern the long-range (pion-exchange) component of the inter-nucleon forces. The first principles calculation of meson-nucleon amplitudes from lattice QCD both compliments experiment and probes the quark mass dependence, enabling studies of the convergence of the asymptotic perturbative series. Low-energy pion-nucleon scattering is also related to the pion-nucleon sigma term $\sigma_{\pi N}$ [1, 2], which is an input to the phenomenology of dark matter direct-detection experiments. Some tension currently exists between lattice determinations of $\sigma_{\pi N}$ and phenomenological extractions of $\sigma_{\pi N}$ from πN scattering data [3], so that precise lattice calculations of the πN scattering lengths are needed. At somewhat larger center-of-mass energy, electroweak form-factors of the $N \rightarrow \Delta(1232) \rightarrow N\pi$ transition are needed for neutrino-nucleus scattering experiments [4], and the nature of the low-lying $N(1440)$ and $\Lambda(1405)$ resonances remain unsettled.

Although lattice QCD is well established as a reliable non-perturbative approach to calculating the properties of single hadrons, lattice QCD studies of hadron scattering amplitudes have proven more difficult. Increased development of the formalism for relating finite-volume lattice observables to infinite-volume amplitudes, the rapid growth of computer power, and novel efficient numerical algorithms have combined to advance the state-of-the-art. This review highlights the substantial recent progress achieved in lattice QCD calculations of hadron scattering amplitudes, in particular on the nascent subfield of meson-nucleon systems. A related review of lattice QCD calculations of meson-baryon scattering amplitudes is given in Ref. [5].

A detailed introduction to lattice QCD is beyond the scope of this work [6, 7], but several main points are worthy of mention. Lattice QCD employs the path integral formulation of QFT regulated on a finite space-time lattice of $(L/a)^3 \times (T/a)$ points, where a denotes the lattice spacing and L (T) the spatial (temporal) extent. After analytically integrating out the quark fields, Markov chain Monte Carlo methods sample the remaining path integral over the gluon field (denoted U) to produce stochastic estimates for Euclidean n -point correlation functions. Employing the time-momentum representation for a correlation function between hadron interpolating fields \mathcal{O}_i and \mathcal{O}_j results in the spectral decomposition

$$C_{ij}^{2\text{pt}}(\mathbf{p}, \tau) = \langle \mathcal{O}_i(\mathbf{p}, \tau) \mathcal{O}_j^\dagger(0) \rangle_U = \sum_n \langle 0 | \hat{\mathcal{O}}_i(\mathbf{p}) | n \rangle \langle n | \hat{\mathcal{O}}_j^\dagger(0) | 0 \rangle e^{-E_n \tau} + \mathcal{O}(e^{-MT}) \quad (1)$$

where $\langle \dots \rangle_U$ denotes the Monte Carlo average over suitably distributed gluon fields and the sum runs over finite-volume Hamiltonian eigenstates $\hat{H}|n\rangle = E_n|n\rangle$. The form of the exponentially suppressed finite- T effects depends on the temporal boundary conditions and the interpolating operators. Evidently the large-time limit of these Euclidean n -point functions is dominated by the lowest contributing eigenstates and analyses of $C_{ij}^{2\text{pt}}(\mathbf{p}, \tau)$ treating the first few terms in the sum enable a determination of the low-lying finite-volume energies and matrix elements [8, 9, 10]. Such determinations are hampered by the exponential signal-to-noise degradation typically present as $\tau \rightarrow \infty$ so that in practice finite-volume levels are isolated successfully only if the employed set of operators $\{\mathcal{O}_i\}$ has significant overlap onto them.

As is evident from Eq. 1, lattice QCD simulations are performed in Euclidean time $\tau = it$. The usual determination of scattering amplitudes in real time relies on an asymptotic formalism, such as the well-known LSZ [11] and Haag-Ruelle [12, 13] approaches, where the asymptotic time limits $t \rightarrow \pm\infty$ of correlation functions isolate the desired in and out states. Although an analogous asymptotic formalism has been proposed for Euclidean time in Ref. [14], Maiani and Testa [15] proved that the naive large-separation limit of Euclidean correlators does not (in general) yield on-shell scattering amplitudes. Fortunately, a work-around was developed by Lüscher [16] in which the finite-volume is used

as a tool to probe hadron interactions. In this approach the signal consists of the deviation of finite-volume two-hadron levels from their non-interacting values. Although originally formulated for total momentum $\mathbf{P} = 0$ elastic scattering between two spinless identical particles, generalizations have been developed for moving frames [17, 18, 19], non-identical particles with spin [20, 21, 22], asymmetric volumes [23], coupled two-hadron scattering channels [24, 25, 26, 27, 28], and amplitudes containing external currents [27, 28, 29, 30, 31, 32, 33, 34, 35, 36, 37, 38, 39, 40]. Although this approach, which is reviewed in Ref. [41], is applicable to two-to-two scattering only below three (or more) hadron thresholds, extensions treating three-hadron amplitudes are under development [42, 43, 44, 45, 46, 47, 48, 49, 50, 51, 52, 53, 54, 55, 56].

Using the notation of Ref. [22], the relation between a finite-volume two-hadron energy $E_L^\Lambda(\mathbf{P})$ and infinite-volume two-to-two scattering amplitudes is given by

$$\det[K^{-1}(E_{\text{cm}}) - B^{(P)}(L, E_{\text{cm}})] + \mathcal{O}(e^{-ML}) = 0, \quad E_{\text{cm}} = \sqrt{(E_L^\Lambda(\mathbf{P}))^2 + \mathbf{P}^2} \quad (2)$$

where the exponentially suppressed corrections are ignored in practical applications and Λ denotes an irreducible representation (irrep) of the relevant finite-volume symmetry group. This ‘quantization condition’ yields information about the infinite-volume K -matrix in the form of a determinant over all possible total angular momenta (J), total spin combinations (S), and two-hadron scattering channels (a). Encoding the reduced symmetry of the cubic volume in lattice QCD simulations, the (known) B -matrix mixes the infinite number of possible J while the K -matrix is diagonal in J but dense in S and a . The practical application of Eq. 2 requires a block diagonalization in the basis of finite-volume irreps, and a truncation to the limited set of contributing partial waves below some maximum orbital angular momentum ℓ_{max} . Only in the single-channel, single-partial wave approximation is there a one-to-one correspondence between $E_L^\Lambda(\mathbf{P})$ and $K^{-1}(E_{\text{cm}})$. In other cases a global fit is performed to all energies resulting in a model-dependent parametrization of $K^{-1}(E_{\text{cm}})$.

We turn now to the lattice QCD calculation of finite-volume two-hadron energies $\{E_L^\Lambda(\mathbf{P})\}$ from the two-point correlation functions in Eq. 1. Correlation functions between two-hadron interpolating operators in which each hadron has definite spatial momentum are most effective in isolating two-hadron states. However, the measurement of such correlation functions on an ensemble of gauge field configurations has long been a computational challenge. Since the Grassmann-valued quark fields are integrated out analytically in the lattice QCD path integral, Wick’s theorem is employed to express hadron correlation functions in terms of quark propagators. On a finite discrete Euclidean lattice, the quark propagators between space-time points x and y is given as the inverse of the large, sparse, ill-conditioned Dirac operator $M^{-1}(x, y)$. This matrix is so large that its inverse is computed only by solving linear systems $M\phi = \eta$ for some ‘sink’ $\phi(x)$ given a ‘source’ $\eta(y)$. Projection onto definite spatial momentum however requires knowledge of the entire matrix inverse, so-called all-to-all quark propagators. The calculation of all required elements of this matrix inverse on each gauge configuration by solving one linear system for each space-time point is prohibitively expensive, so alternative algorithms are required. One approach that has been particularly successful is the Laplacian-Heaviside method (LapH) [57, 58] in which the all-to-all quark propagator is projected onto the subspace spanned by the N_{ev} lowest modes of the gauge covariant Laplace operator, reducing its dimension significantly and enabling the computation of the smeared all-to-all propagator. This method has the added benefits of affecting a form of quark smearing, whereby the overlap onto the high-lying states in Eq. 1 is suppressed, and reducing the problem of correlation function construction to the contraction of individual hadron tensors, for which significant optimizations can be applied [59]. Although the LapH approach still requires a large number of inversions on each gauge configuration, advances in algorithms [60, 61] for solving linear systems involving the Dirac matrix M have improved the computational cost significantly.

Complimentary developments in the finite-volume formalism and in the computation of two-hadron energies in lattice QCD have driven recent progress in calculations of two-hadron scattering amplitudes. Although much of this progress has been in amplitudes with two pseudoscalar mesons, first meson-nucleon calculations have been performed. It is these calculations that are highlighted here, with work on threshold $N\pi$ amplitudes summarized separately from first calculations of the low-lying $\Delta(1232)$ resonance. Finally, a new approach for determining scattering amplitudes for spectral functions *without* employing the finite volume is reviewed, before concluding with a summary and future prospects.

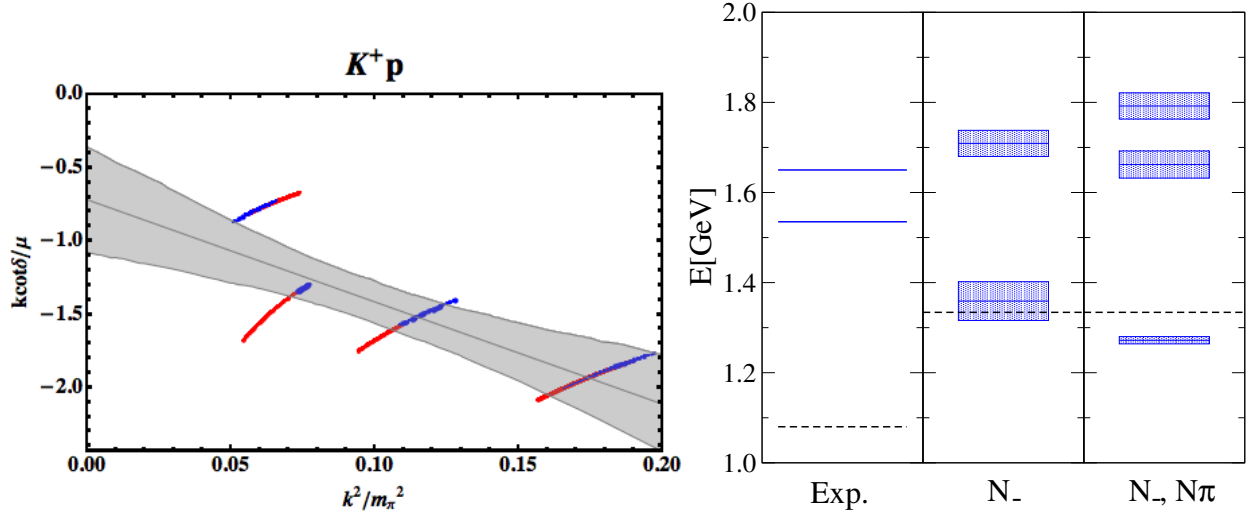


FIGURE 1. *Left:* the low-energy $K^+ p$ scattering amplitude from Ref. [64] on a single ensemble with $N_f = 2 + 1$ dynamical Wilson fermions at pion mass $m_\pi = 390\text{MeV}$. The red and blue points are results on individual bootstrap samples for two different analysis strategies and the gray band is a fit to Eq. 3 including the first two terms in the effective range expansion. *Right:* low-lying finite volume spectrum in the $I = 1/2$ G_{1u} irrep from Ref. [65] on a single $N_f = 2$ ensemble with $m_\pi = 266\text{MeV}$. The first column are the experimentally known $N^*(1535)$ and $N^*(1650)$ resonances and the second column is the lattice QCD finite volume spectrum determined using only single-hadron operators. The third column is the spectrum determined accurately using both single-hadron and $N\pi$ interpolating operators, illustrating the need for a complete basis in practical calculations.

THRESHOLD SCATTERING AMPLITUDES

The natural first application of the methods described above is to near-threshold meson-nucleon amplitudes, where the effective range expansion of $\ell = 0$ partial waves

$$p_{\text{cm}} \cot \delta_0(p_{\text{cm}}) = -\frac{1}{a_0} + \frac{1}{2} r_0 p_{\text{cm}}^2 + P_0 r_0^3 p_{\text{cm}}^4 + \mathcal{O}(p_{\text{cm}}^6) \quad (3)$$

defines the scattering length a_0 , the effective range r_0 , and the shape parameter P_0 . These are of course parametrization-independent constants that characterize the low-energy interaction and thus of phenomenological significance. On the finite-volume formalism side, truncating Eq. 2 to s -wave contributions only yields a one-to-one correspondence between lattice QCD energies and scattering amplitudes. Although not required in practical applications, the threshold expansion of Eq. 2 is instructive and yields

$$\Delta E \equiv E_{mN}^{G_{1g}}(L) - M_m - M_N = \frac{-2\pi a_0}{\mu_{mN} L^3} \left[1 + c_1 \frac{a_0}{L} + c_2 \left(\frac{a_0}{L} \right)^2 \right] + \mathcal{O}\left(\frac{1}{L} \right)^6 \quad (4)$$

where $E_{mN}^{G_{1g}}(L)$ is the finite-volume energy of the lowest lying meson-nucleon energy in the G_{1g} irrep, μ_{mN} the reduced mass of the meson-nucleon system, and c_1 and c_2 are known constants [62]. Eq. 4 illustrates that finite-volume energy shifts indeed constitute the signal for scattering amplitudes, and that sensitivity to higher-order terms in Eq. 3 occurs only at $\mathcal{O}\left(\frac{1}{L}\right)^6$.

Several low-energy s -wave meson-nucleon scattering amplitudes have been calculated using this approach in Refs. [63, 64]. The quantum numbers of the overall system are chosen to ensure the absence of ‘same-time’ diagrams which contain quark propagators that start and end at the same time. Since only a single ground state is determined, projecting onto definite momentum everywhere is not strictly required, although it does enhance the overlap onto the desired level. Refs. [63, 64] exploit these simplifications and do not employ the LapH approach for the required quark propagators. Ref. [64] employs ensembles of $N_f = 2 + 1$ dynamical fermions with a single lattice spacing and pion masses $m_\pi = 390, 250\text{MeV}$. The results for low-energy $K^+ p$ scattering are shown in Fig. 1.

Ref. [65] computes the lowest three $I = 1/2$ $N\pi$ finite-volume energy levels in the G_{1u} irrep for which the leading partial wave approximation yields the near-threshold s -wave amplitude. Since this system has non-maximal isospin,

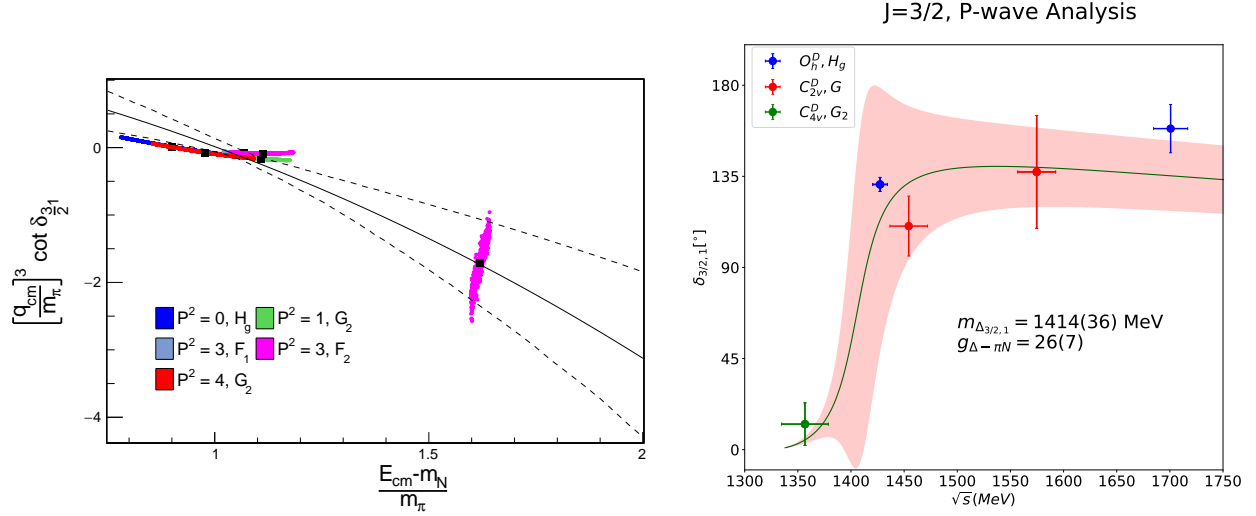


FIGURE 2. *Left:* the elastic $I = 3/2$ p -wave $N\pi$ scattering amplitude from Ref. [66] on a single ensemble of $N_f = 2 + 1$ Wilson fermions with $m_\pi = 280$ MeV. Due to the unphysical values of the quark masses the $\Delta(1232)$ resonance is located near the $N\pi$ threshold. Individual bootstrap samples are shown for each point to illustrate correlations and the lines indicate a Breit-Wigner fit. Ref. [66] also justified the single-partial wave approximation by expanding the determinant condition in Eq. 2 to include all contributing d -waves, finding their contribution negligible. *Right:* Preliminary $I = 3/2$ p -wave $N\pi$ scattering phase shift from Ref. [68] on a single ensemble of $N_f = 2 + 1$ dynamical fermions at $m_\pi = 250$ MeV. The shaded region indicates the error band from a Breit-Wigner fit.

same-time diagrams are required and the LapH method is used to efficiently determine the (smeared) all-to-all quark propagators. Definite three-momentum projection is performed for all hadrons and appropriate interpolators for each of the three lowest-lying states are included. Results for the three finite-volume energy levels for a single ensemble of $N_f = 2$ dynamical fermions with $m_\pi = 266$ MeV are shown in Fig. 1. In this analysis, single-hadron interpolating operators for the lowest-lying resonances in this channel are also included. The importance of appropriate interpolating operators is illustrated by comparison with the lattice spectra obtained with and without the $N\pi$ operator. Due to the exponentially degrading signal-to-noise ratio, there is a finite time range over which the signal can be tracked and the lowest-lying level is determined correctly only if the $N\pi$ is included. Although only the first level is relevant for the near-threshold scattering amplitude, the next two are in qualitative agreement with the experimentally determined $N^*(1535)$ and $N^*(1650)$ resonances.

RESONANT AMPLITUDES

As is evident in Fig. 1, both single-hadron and two-hadron interpolating operators are required to determine the low-lying spectrum in the presence of resonances. Below three or more hadron thresholds, this spectrum can be interpreted according to Eq. 2 to obtain information about meson-nucleon scattering amplitudes above threshold. The benchmark example of such an analysis is the $I = 3/2$ p -wave elastic $N\pi$ scattering amplitude, which contains the narrow $\Delta(1232)$ resonance. This analysis must include single-hadron $\Delta(1232)$ interpolating operators as well as $N\pi$ operators with appropriate overall quantum numbers.

The first published results on the $\Delta(1232)$ resonance appeared in Ref. [66], although a report on preliminary earlier work is found in Ref. [67]. Ref. [66] employs a single ensemble of $N_f = 2 + 1$ dynamical quarks at $m_\pi = 280$ MeV which lies on a quark mass trajectory that fixes $2m_{u,d} + m_s = \text{const.}$ to the physical value. Because the degenerate light quark masses are larger than their physical values, the $\Delta(1232)$ is approximately stable and located near $E_{\text{thresh}} = m_N + m_\pi$. This hampers a determination of the energy dependence of the amplitude, as is evident in Fig. 2. Nonetheless, a Breit-Wigner fit to $p^3 \cot \delta$ yields $m_\Delta = 1344(20)$ MeV and $g_{\Delta N \pi}^{\text{BW}} = 19.0(7.4)$ which are consistent with phenomenological determinations from experimental data. Although Ref. [66] employs the single partial wave approximation, the influence of d -waves is checked explicitly by enlarging the determinant in Eq. 2 using the formulae and computer programs published in Ref. [22].

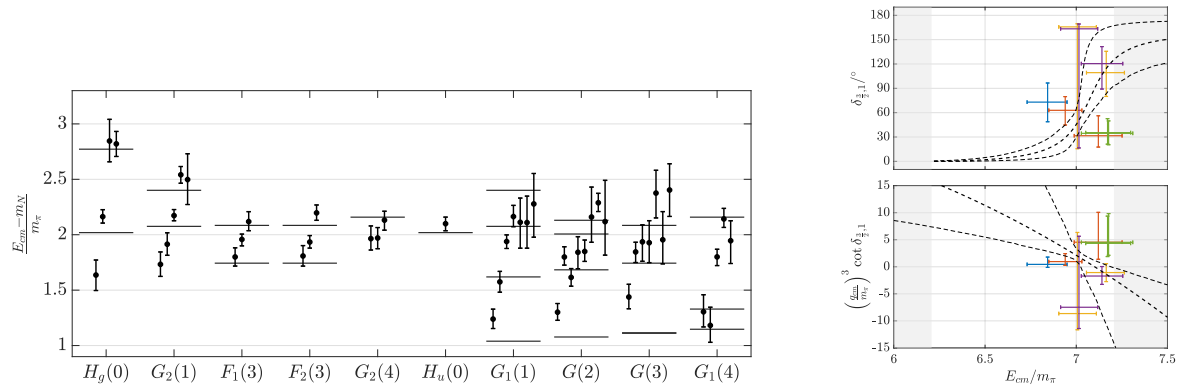


FIGURE 3. From Ref. [70], preliminary results for the elastic $I = 3/2$ p -wave $N\pi$ scattering amplitude on a single ensemble of $N_f = 2 + 1$ dynamical fermions at $m_\pi = 200\text{MeV}$. *Left:* the finite volume spectra in irreps containing both s - and p -wave contributions. *Right:* a plot of p -wave dominated irreps for which the single-partial wave approximation is applied together with a Breit-Wigner fit to all levels where the s -wave is modeled by a constant.

Preliminary results on the $\Delta(1232)$ resonance are also found in Ref. [68] on a single ensemble of $N_f = 2 + 1$ dynamical fermions at $m_\pi = 250\text{MeV}$. There the leading partial wave approximation is applied and all necessary Wick contractions are evaluated using a combination of sequential, stochastic and point-to-all propagators. Preliminary results from Ref. [68] are also shown in Fig. 2, which result in a value of the coupling $g_{\Delta N\pi}$ compatible with Ref. [66] and the preliminary determination in Ref. [69].

In both Refs. [66] and [68] energies are calculated in a number of kinematic frames, but with finite-volume irreps judiciously chosen so that $\ell = 1$ is the lowest contributing infinite-volume partial wave. In a number of other irreps, both s - and p -waves contribute, enabling a larger number of constraints on the K -matrix due to the increased number of finite-volume energies. However, a more complicated analysis is required where s - and p -waves are fit simultaneously to Eq. 2. First preliminary results from an analysis of this type [70] are shown in Fig. 3 on a single ensemble of $N_f = 2 + 1$ dynamical fermions at $m_\pi = 200\text{MeV}$. Evidently, the inclusion of s - and p -wave dominated irreps provides a number of additional finite-volume energy levels which better constrain the p -wave Breit-Wigner fit parameters. The s -wave is modeled using the leading term in the effective range expansion from Eq. 3.

SCATTERING FROM SPECTRAL FUNCTIONS

Although it continues to be successful where applicable, the finite-volume formalism employed above has several shortcomings. Chiefly among them is the restriction of Eq. 2 to energies below three (or more) hadron thresholds, preventing the study of many interesting systems including excited nucleon resonances. If the three-hadron formalism is fully developed and applied, finite-volume energy levels up to four (or more) hadron thresholds may be interpreted, but no general approach exists for levels above arbitrary inelastic thresholds. Further limitations of the finite-volume formalism include the inability to directly calculate inclusive rates such as the purely hadronic process $p + p \rightarrow X$, where X denotes a sum over all hadronic final states.

An alternative approach to determining real-time scattering amplitudes from Euclidean correlation functions is motivated by expressing the two-point correlation function in Eq. 1 as

$$C_{ij}(\mathbf{p}, \tau) = \int_0^\infty dE \rho_{ij}(\mathbf{p}, E) e^{-E\tau}, \quad \rho_{ij}(\mathbf{p}, E) = \sum_n \delta(E - E_n) \langle 0 | \hat{\mathcal{O}}_i(\mathbf{p}) | n \rangle \langle n | \hat{\mathcal{O}}_j^\dagger(0) | 0 \rangle \quad (5)$$

in terms of the spectral function $\rho_{ij}(\mathbf{p}, E)$. These spectral functions are independent of the metric signature and therefore contain real-time information. However, $C_{ij}(\mathbf{p}, \tau)$ is determined from the lattice Monte Carlo calculation at a finite number of τ , each with a statistical error. The reconstruction of $\rho_{ij}(\mathbf{p}, E)$ from such data is therefore an ill-posed problem.

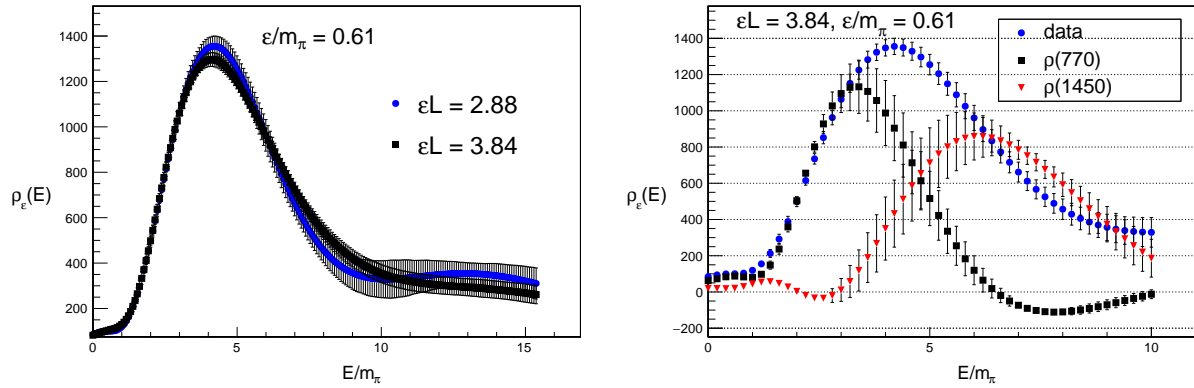


FIGURE 4. Spectral reconstruction of the smeared isovector vector correlator from Ref. [81] for $N_f = 2 + 1$ dynamical fermions at $m_\pi = 220\text{MeV}$ and $a = 0.086\text{fm}$. *Left:* $\rho_\varepsilon(E)$ at two volumes illustrating the rapid onset of the infinite volume limit at fixed ε . *Right:* Individual state contributions of a fit to the data to Eq. 8 with $N_{\text{pole}} = 2$ resulting in energies consistent with the $\rho(770)$ and the $\rho(1450)$.

A more modest goal is the determination of the smeared spectral function

$$\rho_{ij}^\varepsilon(\mathbf{p}, E) = \int_0^\infty d\omega \delta_\varepsilon(E - \omega), \quad \lim_{\varepsilon \rightarrow 0^+} \delta_\varepsilon(x) = \delta(x) \quad (6)$$

where the smearing kernel $\delta_\varepsilon(E - \omega)$ approaches a Dirac- δ function as the smearing width is reduced. While the smearing is a necessary limitation introduced by the nature of the problem, it is advantageous in bridging the gap between finite and infinite volume. Although unsmearing spectral functions are very different in finite and infinite volume, at finite (fixed) smearing width ε the infinite-volume limit is well defined. Furthermore, recent improvements [71] to the Backus-Gilbert algorithm [72, 73] for spectral reconstruction enable the efficient determination of ρ^ε with an input functional form for the smearing kernel $\delta_\varepsilon(E - \omega)$. These methods provide the exact smeared spectral function, but smeared with a (known) smearing kernel $\hat{\delta}_\varepsilon(E, \omega)$ that is only approximately equal to the desired one $\delta_\varepsilon(E - \omega)$. An ideal choice for the smearing kernel [74, 75] is the real part of the standard $i\varepsilon$ -prescription for causal propagation

$$\pi \delta_\varepsilon(E - \omega) = \text{Re} \frac{i}{E - \omega + i\varepsilon} = \frac{\varepsilon}{(E - \omega)^2 + \varepsilon^2}. \quad (7)$$

which has desirable analyticity properties in ε , unlike (for instance) a gaussian smearing kernel. Physical on-shell scattering amplitudes are then obtained from the ordered double limit $\lim_{\varepsilon \rightarrow 0^+} \lim_{L \rightarrow \infty}$. This approach was proposed first for inclusive processes mediated by external currents in Ref. [76] and extended to arbitrary scattering amplitudes in Ref. [74].

As an illustrative application, consider the total rate for the inclusive process $\hat{J} \rightarrow \text{hadrons}$, which \hat{J} is an external current. An example of such a process is the ratio $R_{\text{had}}(s) = \sigma(e^+e^- \rightarrow \text{hadrons}) / \frac{4\pi\alpha_{\text{em}}(s)}{3s}$ with the electromagnetic external current, which is relevant for the phenomenology of $(g-2)_\mu$ [77]. Fictitious inclusive processes can also be considered, in which the currents do not correspond to real-world external probes, but can be an arbitrary hadronic interpolator $\hat{\mathcal{O}}_{\text{had}}$. In order for such processes to act as novel probes of QCD, these hadronic interpolators must be renormalized to possess a well-defined continuum limit. The renormalization of arbitrary hadron interpolators can be accomplished either using the Wilson flow [78, 79] or the approach of Ref. [80], but indicative preliminary results are shown with a smeared unrenormalized $I = 1$ vector current in Fig. 4. There the inclusive rate $\sigma(\hat{\mathcal{O}}_{\text{had}} \rightarrow \text{hadrons})(E) \propto \lim_{\varepsilon \rightarrow 0^+} \rho_\varepsilon(E)$ is determined at finite ε and multiple volumes using the freely-available lattice correlator data from Ref. [81].

Two different spatial volumes illustrate the rapid approach to the $L \rightarrow \infty$ limit at finite ε , so that an infinite-volume *ansatz* for $\rho_\varepsilon(E)$ is appropriate. In this channel peaks associated with the $\rho(770)$ resonance as well as excited $I^G(J^P) = 1^+(1^-)$ resonances are expected. However, the smearing width $\varepsilon = 0.61m_\pi = 135\text{MeV}$ is larger than the typical width of these states so that an *ansatz* that treats them as infinitesimally narrow is appropriate. To fit $\rho_\varepsilon(E)$, we employ the

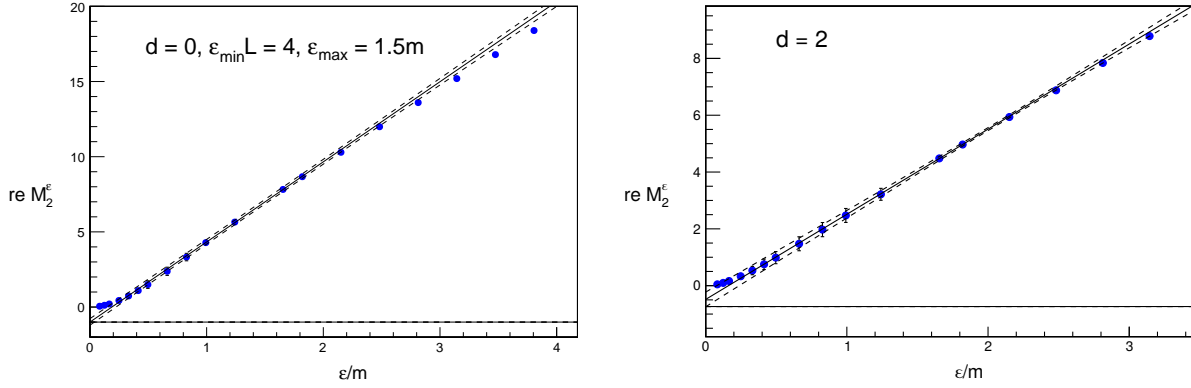


FIGURE 5. Preliminary results for the real part of the elastic $I = 2$ two-to-two scattering amplitude in the 1+1 dimensional $O(3)$ model with $mL = 19.4$. For zero total momentum, results for $M_2^\epsilon(E^*)$ from Eq. are shown for zero units of relative momentum (*left*) and two units of relative momentum (*right*). For each case, the order double limit is performed by extrapolating linearly to $\epsilon \rightarrow 0$ over the range $[\epsilon_{\min}, \epsilon_{\max}]$. The horizontal solid line corresponds to the exact results from Refs. [9, 83], which is consistent with the extrapolated values. Deviations from linearity are evident for $\epsilon < \epsilon_{\min}$ illustrating the importance of the ordered double limit.

model

$$\rho_\epsilon(E) = \sum_{n=1}^{N_{\text{pole}}} A_n \delta(E - E_n) \quad (8)$$

to describe the data in Fig. 4. The $N_{\text{pole}} = 1$ form does not provide a good description of the data, resulting in an (uncorrelated) $\chi^2/\text{d.o.f.} = 42.8$, but using the four-parameter $N_{\text{pole}} = 2$ *ansatz* reduces this to $\chi^2/\text{d.o.f.} = 0.65$. The resultant energies in this fit are $E_1 = 740(30)\text{MeV}$ and $E_2 = 1394(109)\text{MeV}$ which are consistent with the experimentally determined masses of the $\rho(770)$ and $\rho(1450)$.

While this inclusive example models the smeared total rate at finite ϵ , exclusive amplitudes can be recovered in the $\epsilon \rightarrow 0^+$ limit using the LSZ reduction approach of Ref. [74]. As a first demonstration of using spectral functions to obtain exclusive amplitudes [82], consider the 1 + 1-dimensional $O(3)$ model employed in Ref. [9]. Like QCD, this model is asymptotically free and has a mass gap, but the elastic two-to-two scattering amplitude is known analytically [83] so it is an ideal test case. Furthermore the global $O(3)$ symmetry is reminiscent of isospin symmetry in QCD, so that two-to-two scattering proceeds in one of three ‘isospin’ channels with $I = 0, 1, 2$.

In order to calculate the two-to-two scattering amplitude using the LSZ reduction approach, the connected Euclidean four-point temporal correlation function is computed and the two outer time separations are taken asymptotically large. The resultant correlation function has a single Euclidean time argument, to which the spectral reconstruction of Eqs. 5 and 6 is applied to obtain the smeared spectral function $\rho_{\epsilon(E)}$. The two-to-two scattering amplitude $M_2(E^*)$ is then computed from the ordered double limit

$$M_2(E^*) = \lim_{\epsilon \rightarrow 0^+} \lim_{L \rightarrow \infty} M_2^\epsilon(E^*), \quad M_2^\epsilon(E^*) = Z^{-1} \epsilon^2 \rho_\epsilon(E^*) \quad (9)$$

where E^* is the total (lab frame) energy and Z the interpolator overlap factor. Note the factor of ϵ^2 which performs the ‘amputation’ of the on-shell pole. Since only the real part of the amplitude is considered here, the smearing kernel from Eq. 7 is employed.

The double limit in Eq. is performed numerically in Fig. 5 at a fixed $mL = 19.4$ by extrapolating linearly to $\epsilon = 0$ using data in the range $\epsilon_{\min} < \epsilon < \epsilon_{\max}$, with $\epsilon_{\min}L = 4$ to remain safe from finite-volume effects and $\epsilon_{\max} = 1.5m$ to remain in the linear regime. As is evident in Fig. 5, this extrapolation results in scattering amplitudes consistent with the known analytic result. Deviations from linearity are also apparent in Fig. 5 for $\epsilon < \epsilon_{\min}$, which illustrate the need for the appropriate ordered double limit.

CONCLUSIONS

This review surveys the current state of lattice QCD calculations of meson-nucleon scattering amplitudes, which is an emerging subfield. The finite-volume formalism of Eq. 2 has been successful in first calculations of two-to-two amplitudes below three or more hadron thresholds. These include near-threshold studies which determine parameters of the effective range expansion as well as first studies of the $\Delta(1232)$ resonance across the entire elastic region. All meson-nucleon calculations to date have also treated only elastic scattering, although Eq. 2 applies also to coupled two-hadron scattering channels which are relevant for the $\Lambda(1405)$ resonance. Furthermore, extension of the finite-volume formalism to treat meson-meson-baryon channels and the corresponding lattice QCD computation of the spectra have not yet been completed, although first calculations of three-pion scattering amplitudes are encouraging [59, 84, 85]. Nonetheless, the range of impact of the two-to-two scattering amplitudes can be increased by using lattice QCD scattering data as an input to effective field theories and EFT-inspired models. Work in this direction with nucleons has already been performed [86, 87].

In general progress in meson-baryon scattering on the lattice has been slower than meson-meson calculations due to several difficulties, such as the increased signal-to-noise problem, complications in correlator construction due to the extra quark, and complications in the finite-volume formalism from the inclusion of non-identical particles with non-zero overall spin. Despite these difficulties, it is reasonable to assume that (in analogy with the meson-meson sector) precise results for elastic amplitudes and coupled meson-baryon scattering channels will be produced in the near future. Making further comparisons with meson scattering amplitudes, it is likely that calculations of meson-baryon amplitudes mediated by external electroweak currents \hat{J}_{ew} are also possible, such as $N + J_{\text{ew}} \rightarrow N + \pi$ and $N + \pi + J_{\text{ew}} \rightarrow N + \pi$, which have a number of phenomenological applications. There has been substantial progress on analogous amplitudes in the meson-meson sector, such as $\gamma^* \rightarrow \pi\pi$ in Refs. [36, 81] and $\pi + \gamma^* \rightarrow \pi\pi$ in Refs. [88, 89].

The final topic discussed in this review is a novel approach to computing scattering amplitudes in lattice QCD simulations based on spectral functions. This does not employ the finite volume whatsoever and as such requires large volumes to saturate the $L \rightarrow \infty$ limit. Because of this, larger volumes are required than in typical lattice QCD simulations, although some preliminary indicative results for inclusive decays on existing lattice QCD data are encouraging. The LSZ reduction approach of Ref. [74] has not yet been employed in lattice QCD but preliminary results in a 1+1 dimensional toy model reproduce the known elastic two-to-two scattering amplitude. Overall, if feasible the infinite-volume formalism based on spectral functions has the potential to circumvent many of the limitations present when using the finite-volume, such as partial wave and coupled-channel mixing as well as the difficulty in going above arbitrary inelastic thresholds. These issues are of course relevant when studying excited nucleon resonances. However, the degree to which Refs. [74] and [76] can be applied to lattice QCD simulation data is an open question.

REFERENCES

1. T. P. Cheng and R. F. Dashen, "Is SU(2) x SU(2) a better symmetry than SU(3)?" Phys. Rev. Lett. **26**, 594 (1971).
2. L. S. Brown, W. J. Pardee, and R. D. Peccei, "Adler-Weisberger theorem reexamined," Phys. Rev. **D4**, 2801–2810 (1971).
3. J. Ruiz de Elvira, M. Hoferichter, B. Kubis, and U.-G. Meißner, "Extracting the σ -term from low-energy pion-nucleon scattering," J. Phys. **G45**, 024001 (2018), arXiv:1706.01465 [hep-ph].
4. L. Alvarez-Ruso *et al.*, "NuSTEC White Paper: Status and challenges of neutrino–nucleus scattering," Prog. Part. Nucl. Phys. **100**, 1–68 (2018), arXiv:1706.03621 [hep-ph].
5. C. Morningstar, "Recent highlights with baryons from lattice QCD," (2019) arXiv:1909.08145 [nucl-th].
6. C. Gattringer and C. B. Lang, "Quantum chromodynamics on the lattice," Lect. Notes Phys. **788**, 1–343 (2010).
7. T. DeGrand and C. E. Detar, *Lattice methods for quantum chromodynamics* (2006).
8. C. Michael, "Adjoint Sources in Lattice Gauge Theory," Nucl. Phys. **B259**, 58–76 (1985).
9. M. Luscher and U. Wolff, "How to Calculate the Elastic Scattering Matrix in Two-dimensional Quantum Field Theories by Numerical Simulation," Nucl. Phys. **B339**, 222–252 (1990).
10. B. Blossier, M. Della Morte, G. von Hippel, T. Mendes, and R. Sommer, "On the generalized eigenvalue method for energies and matrix elements in lattice field theory," JHEP **04**, 094 (2009), arXiv:0902.1265 [hep-lat].
11. H. Lehmann, K. Symanzik, and W. Zimmermann, "Zur formulierung quantisierter feldtheorien," Il Nuovo Cimento (1955-1965) **1**, 205–225 (1955).
12. R. Haag, "Quantum Field Theories with Composite Particles and Asymptotic Conditions," Physical Review **112**, 669–673 (1958).
13. D. Ruelle, "On the asymptotic condition in quantum field theory," Helv. Phys. Acta **35** (1962).
14. J. C. A. Barata and K. Fredenhagen, "Particle scattering in Euclidean lattice field theories," Commun. Math. Phys. **138**, 507–520 (1991).
15. L. Maiani and M. Testa, "Final state interactions from Euclidean correlation functions," Phys. Lett. **B245**, 585–590 (1990).
16. M. Lüscher, "Two particle states on a torus and their relation to the scattering matrix," Nucl. Phys. **B354**, 531–578 (1991).

17. K. Rummukainen and S. A. Gottlieb, “Resonance scattering phase shifts on a nonrest frame lattice,” Nucl. Phys. **B450**, 397–436 (1995), arXiv:hep-lat/9503028 [hep-lat].
18. C. h. Kim, C. T. Sachrajda, and S. R. Sharpe, “Finite-volume effects for two-hadron states in moving frames,” Nucl. Phys. **B727**, 218–243 (2005), arXiv:hep-lat/0507006 [hep-lat].
19. Z. Fu, “Rummukainen-Gottlieb’s formula on two-particle system with different mass,” Phys. Rev. **D85**, 014506 (2012), arXiv:1110.0319 [hep-lat].
20. M. Göckeler, R. Horsley, M. Lage, U. G. Meißner, P. E. L. Rakow, A. Rusetsky, G. Schierholz, and J. M. Zanotti, “Scattering phases for meson and baryon resonances on general moving-frame lattices,” Phys. Rev. **D86**, 094513 (2012), arXiv:1206.4141 [hep-lat].
21. R. A. Briceño, “Two-particle multichannel systems in a finite volume with arbitrary spin,” Phys. Rev. **D89**, 074507 (2014), arXiv:1401.3312 [hep-lat].
22. C. Morningstar, J. Bulava, B. Singha, R. Brett, J. Fallica, A. Hanlon, and B. Hörz, “Estimating the two-particle K -matrix for multiple partial waves and decay channels from finite-volume energies,” Nucl. Phys. **B924**, 477–507 (2017), arXiv:1707.05817 [hep-lat].
23. X. Feng, X. Li, and C. Liu, “Two particle states in an asymmetric box and the elastic scattering phases,” Phys. Rev. **D70**, 014505 (2004), arXiv:hep-lat/0404001 [hep-lat].
24. S. He, X. Feng, and C. Liu, “Two particle states and the S -matrix elements in multi-channel scattering,” JHEP **07**, 011 (2005), arXiv:hep-lat/0504019 [hep-lat].
25. M. Lage, U.-G. Meißner, and A. Rusetsky, “A Method to measure the antikaon-nucleon scattering length in lattice QCD,” Phys. Lett. **B681**, 439–443 (2009), arXiv:0905.0069 [hep-lat].
26. V. Bernard, M. Lage, U. G. Meißner, and A. Rusetsky, “Scalar mesons in a finite volume,” JHEP **01**, 019 (2011), arXiv:1010.6018 [hep-lat].
27. R. A. Briceño and Z. Davoudi, “Moving multichannel systems in a finite volume with application to proton-proton fusion,” Phys. Rev. **D88**, 094507 (2013), arXiv:1204.1110 [hep-lat].
28. M. T. Hansen and S. R. Sharpe, “Multiple-channel generalization of Lellouch-Lüscher formula,” Phys. Rev. **D86**, 016007 (2012), arXiv:1204.0826 [hep-lat].
29. L. Lellouch and M. Lüscher, “Weak transition matrix elements from finite volume correlation functions,” Commun. Math. Phys. **219**, 31–44 (2001), arXiv:hep-lat/0003023 [hep-lat].
30. C. J. D. Lin, G. Martinelli, C. T. Sachrajda, and M. Testa, “ $K \rightarrow \pi \pi$ decays in a finite volume,” Nucl. Phys. **B619**, 467–498 (2001), arXiv:hep-lat/0104006 [hep-lat].
31. W. Detmold and M. J. Savage, “Electroweak matrix elements in the two nucleon sector from lattice QCD,” Nucl. Phys. **A743**, 170–193 (2004), arXiv:hep-lat/0403005 [hep-lat].
32. H. B. Meyer, “Lattice QCD and the Timelike Pion Form Factor,” Phys. Rev. Lett. **107**, 072002 (2011), arXiv:1105.1892 [hep-lat].
33. V. Bernard, D. Hoja, U. G. Meißner, and A. Rusetsky, “Matrix elements of unstable states,” JHEP **09**, 023 (2012), arXiv:1205.4642 [hep-lat].
34. W. Detmold and M. Flynn, “Finite-volume matrix elements in multiboson states,” Phys. Rev. **D91**, 074509 (2015), arXiv:1412.3895 [hep-lat].
35. A. Agadjanov, V. Bernard, U. G. Meißner, and A. Rusetsky, “A framework for the calculation of the $\Delta N \gamma^*$ transition form factors on the lattice,” Nucl. Phys. **B886**, 1199–1222 (2014), arXiv:1405.3476 [hep-lat].
36. X. Feng, S. Aoki, S. Hashimoto, and T. Kaneko, “Timelike pion form factor in lattice QCD,” Phys. Rev. **D91**, 054504 (2015), arXiv:1412.6319 [hep-lat].
37. R. A. Briceño, M. T. Hansen, and A. Walker-Loud, “Multichannel $1 \rightarrow 2$ transition amplitudes in a finite volume,” Phys. Rev. **D91**, 034501 (2015), arXiv:1406.5965 [hep-lat].
38. R. A. Briceño and M. T. Hansen, “Multichannel $0 \rightarrow 2$ and $1 \rightarrow 2$ transition amplitudes for arbitrary spin particles in a finite volume,” Phys. Rev. **D92**, 074509 (2015), arXiv:1502.04314 [hep-lat].
39. R. A. Briceño and M. T. Hansen, “Relativistic, model-independent, multichannel $2 \rightarrow 2$ transition amplitudes in a finite volume,” Phys. Rev. **D94**, 013008 (2016), arXiv:1509.08507 [hep-lat].
40. A. Baroni, R. A. Briceño, M. T. Hansen, and F. G. Ortega-Gama, “Form factors of two-hadron states from a covariant finite-volume formalism,” (2018), arXiv:1812.10504 [hep-lat].
41. R. A. Briceño, J. J. Dudek, and R. D. Young, “Scattering processes and resonances from lattice QCD,” Rev. Mod. Phys. **90**, 025001 (2018), arXiv:1706.06223 [hep-lat].
42. R. A. Briceño and Z. Davoudi, “Three-particle scattering amplitudes from a finite volume formalism,” Phys. Rev. **D87**, 094507 (2013), arXiv:1212.3398 [hep-lat].
43. K. Polejaeva and A. Rusetsky, “Three particles in a finite volume,” Eur. Phys. J. **A48**, 67 (2012), arXiv:1203.1241 [hep-lat].
44. M. T. Hansen and S. R. Sharpe, “Relativistic, model-independent, three-particle quantization condition,” Phys. Rev. **D90**, 116003 (2014), arXiv:1408.5933 [hep-lat].
45. U.-G. Meißner, G. Rios, and A. Rusetsky, “Spectrum of three-body bound states in a finite volume,” Phys. Rev. Lett. **114**, 091602 (2015), [Erratum: Phys. Rev. Lett.117,no.6,069902(2016)], arXiv:1412.4969 [hep-lat].
46. M. T. Hansen and S. R. Sharpe, “Expressing the three-particle finite-volume spectrum in terms of the three-to-three scattering amplitude,” Phys. Rev. **D92**, 114509 (2015), arXiv:1504.04248 [hep-lat].
47. R. A. Briceño, M. T. Hansen, and S. R. Sharpe, “Relating the finite-volume spectrum and the two-and-three-particle S matrix for relativistic systems of identical scalar particles,” Phys. Rev. **D95**, 074510 (2017), arXiv:1701.07465 [hep-lat].
48. M. Mai and M. Döring, “Three-body Unitarity in the Finite Volume,” Eur. Phys. J. **A53**, 240 (2017), arXiv:1709.08222 [hep-lat].
49. H.-W. Hammer, J.-Y. Pang, and A. Rusetsky, “Three-particle quantization condition in a finite volume: 1. The role of the three-particle force,” JHEP **09**, 109 (2017), arXiv:1706.07700 [hep-lat].
50. H. W. Hammer, J. Y. Pang, and A. Rusetsky, “Three particle quantization condition in a finite volume: 2. general formalism and the analysis of data,” JHEP **10**, 115 (2017), arXiv:1707.02176 [hep-lat].
51. M. Döring, H. W. Hammer, M. Mai, J. Y. Pang, A. Rusetsky, and J. Wu, “Three-body spectrum in a finite volume: the role of cubic symmetry,” Phys. Rev. **D97**, 114508 (2018), arXiv:1802.03362 [hep-lat].
52. M. Mai and M. Döring, “Finite-Volume Spectrum of $\pi^+ \pi^+$ and $\pi^+ \pi^+ \pi^+$ Systems,” Phys. Rev. Lett. **122**, 062503 (2019), arXiv:1807.04746 [hep-lat].
53. R. A. Briceño, M. T. Hansen, and S. R. Sharpe, “Three-particle systems with resonant subprocesses in a finite volume,” (2018),

- arXiv:1810.01429 [hep-lat].
54. F. Romero-López, A. Rusetsky, and C. Urbach, “Two- and three-body interactions in ϕ^4 theory from lattice simulations,” *Eur. Phys. J.* **C78**, 846 (2018), arXiv:1806.02367 [hep-lat].
 55. M. T. Hansen and S. R. Sharpe, “Lattice QCD and Three-particle Decays of Resonances,” (2019), 10.1146/annurev-nucl-101918-023723, arXiv:1901.00483 [hep-lat].
 56. T. D. Blanton, F. Romero-López, and S. R. Sharpe, “Implementing the three-particle quantization condition including higher partial waves,” (2019), arXiv:1901.07095 [hep-lat].
 57. M. Peardon, J. Bulava, J. Foley, C. Morningstar, J. Dudek, R. G. Edwards, B. Joo, H.-W. Lin, D. G. Richards, and K. J. Juge (Hadron Spectrum), “A Novel quark-field creation operator construction for hadronic physics in lattice QCD,” *Phys. Rev.* **D80**, 054506 (2009), arXiv:0905.2160 [hep-lat].
 58. C. Morningstar, J. Bulava, J. Foley, K. J. Juge, D. Lenkner, M. Peardon, and C. H. Wong, “Improved stochastic estimation of quark propagation with Laplacian Heaviside smearing in lattice QCD,” *Phys. Rev.* **D83**, 114505 (2011), arXiv:1104.3870 [hep-lat].
 59. B. Hörz and A. Hanlon, “Two- and three-pion finite-volume spectra at maximal isospin from lattice QCD,” (2019), arXiv:1905.04277 [hep-lat].
 60. M. Luscher, “Local coherence and deflation of the low quark modes in lattice QCD,” *JHEP* **07**, 081 (2007), arXiv:0706.2298 [hep-lat].
 61. R. Babich, J. Brannick, R. C. Brower, M. A. Clark, T. A. Manteuffel, S. F. McCormick, J. C. Osborn, and C. Rebbi, “Adaptive multigrid algorithm for the lattice Wilson-Dirac operator,” *Phys. Rev. Lett.* **105**, 201602 (2010), arXiv:1005.3043 [hep-lat].
 62. M. Luscher, “Volume Dependence of the Energy Spectrum in Massive Quantum Field Theories. 2. Scattering States,” *Commun. Math. Phys.* **105**, 153–188 (1986).
 63. A. Torok, S. R. Beane, W. Detmold, T. C. Luu, K. Orginos, A. Parreno, M. J. Savage, and A. Walker-Loud, “Meson-Baryon Scattering Lengths from Mixed-Action Lattice QCD,” *Phys. Rev.* **D81**, 074506 (2010), arXiv:0907.1913 [hep-lat].
 64. W. Detmold and A. Nicholson, “Low energy scattering phase shifts for meson-baryon systems,” *Phys. Rev.* **D93**, 114511 (2016), arXiv:1511.02275 [hep-lat].
 65. C. Lang and V. Verduci, “Scattering in the πN negative parity channel in lattice QCD,” *Phys. Rev.* **D87**, 054502 (2013), arXiv:1212.5055.
 66. C. W. Andersen, J. Bulava, B. Hörz, and C. Morningstar, “Elastic $I = 3/2$, p -wave nucleon-pion scattering amplitude and the $\Delta(1232)$ resonance from $N_f=2+1$ lattice QCD,” *Phys. Rev.* **D97**, 014506 (2018), arXiv:1710.01557 [hep-lat].
 67. D. Mohler, “Review of lattice studies of resonances,” *Proceedings, 30th International Symposium on Lattice Field Theory (Lattice 2012): Cairns, Australia, June 24-29, 2012*, PoS **LATTICE2012**, 003 (2012), arXiv:1211.6163 [hep-lat].
 68. S. Paul *et al.*, “Towards the P-wave nucleon-pion scattering amplitude in the $\Delta(1232)$ channel,” *Proceedings, 36th International Symposium on Lattice Field Theory (Lattice 2018): East Lansing, MI, United States, July 22-28, 2018*, PoS **LATTICE2018**, 089 (2018), arXiv:1812.01059 [hep-lat].
 69. V. Verduci, *Pion-nucleon scattering in lattice QCD*, Ph.D. thesis, Graz U. (2014).
 70. C. W. Andersen, J. Bulava, B. Hörz, and C. Morningstar, In prep.
 71. M. Hansen, A. Lupo, and N. Tantalo, “Extraction of spectral densities from lattice correlators,” *Phys. Rev.* **D99**, 094508 (2019), arXiv:1903.06476 [hep-lat].
 72. G. Backus and F. Gilbert, “The resolving power of gross earth data,” *Geophysical Journal International* **16**, 169–205 (1968).
 73. G. Backus and F. Gilbert, “Uniqueness in the inversion of inaccurate gross earth data,” *Philosophical Transactions of the Royal Society of London A: Mathematical, Physical and Engineering Sciences* **266**, 123–192 (1970), <http://rsta.royalsocietypublishing.org/content/266/1173/123.full.pdf>.
 74. J. Bulava and M. T. Hansen, “Scattering amplitudes from finite-volume spectral functions,” *Phys. Rev.* **D100**, 034521 (2019), arXiv:1903.11735 [hep-lat].
 75. E. C. Poggio, H. R. Quinn, and S. Weinberg, “Smearing the Quark Model,” *Phys. Rev.* **D13**, 1958 (1976).
 76. M. T. Hansen, H. B. Meyer, and D. Robaina, “From deep inelastic scattering to heavy-flavor semileptonic decays: Total rates into multihadron final states from lattice QCD,” *Phys. Rev.* **D96**, 094513 (2017), arXiv:1704.08993 [hep-lat].
 77. F. Jegerlehner and A. Nyffeler, “The Muon $g-2$,” *Phys. Rept.* **477**, 1–110 (2009), arXiv:0902.3360 [hep-ph].
 78. M. Lüscher, “Properties and uses of the Wilson flow in lattice QCD,” *JHEP* **08**, 071 (2010), [Erratum: *JHEP*03,092(2014)], arXiv:1006.4518 [hep-lat].
 79. M. Luscher, “Chiral symmetry and the Yang–Mills gradient flow,” *JHEP* **04**, 123 (2013), arXiv:1302.5246 [hep-lat].
 80. M. Papinutto, F. Scardino, and S. Schaefer, “New extended interpolating fields built from three-dimensional fermions,” *Phys. Rev.* **D98**, 094506 (2018), arXiv:1807.08714 [hep-lat].
 81. C. Andersen, J. Bulava, B. Hörz, and C. Morningstar, “The $I = 1$ pion-pion scattering amplitude and timelike pion form factor from $N_f = 2 + 1$ lattice QCD,” *Nucl. Phys.* **B939**, 145–173 (2019), arXiv:1808.05007 [hep-lat].
 82. J. Bulava, M. T. Hansen, M. Hansen, M. W. Hansen, A. Patella, and N. Tantalo, In prep.
 83. A. B. Zamolodchikov and A. B. Zamolodchikov, “Relativistic Factorized S Matrix in Two-Dimensions Having $O(N)$ Isotopic Symmetry,” *Nucl. Phys.* **B133**, 525 (1978), [JETP Lett.26,457(1977)].
 84. T. D. Blanton, F. Romero-López, and S. R. Sharpe, “ $I = 3$ three-pion scattering amplitude from lattice QCD,” (2019), arXiv:1909.02973 [hep-lat].
 85. M. Mai, M. Döring, C. Culver, and A. Alexandru, “Three-body unitarity versus finite-volume $\pi^+ \pi^+ \pi^+$ spectrum from lattice QCD,” (2019), arXiv:1909.05749 [hep-lat].
 86. M. F. M. Lutz, Y. Heo, and X.-Y. Guo, “On the convergence of the chiral expansion for the baryon ground-state masses,” *Nucl. Phys.* **A977**, 146–207 (2018), arXiv:1801.06417 [hep-lat].
 87. Z.-W. Liu, W. Kamleh, D. B. Leinweber, F. M. Stokes, A. W. Thomas, and J.-J. Wu, “Hamiltonian effective field theory study of the $N^*(1440)$ resonance in lattice QCD,” *Phys. Rev.* **D95**, 034034 (2017), arXiv:1607.04536 [nucl-th].
 88. R. A. Briceño, J. J. Dudek, R. G. Edwards, C. J. Shultz, C. E. Thomas, and D. J. Wilson, “The $\pi\pi \rightarrow \pi\gamma^*$ amplitude and the resonant $\rho \rightarrow \pi\gamma^*$ transition from lattice QCD,” *Phys. Rev.* **D93**, 114508 (2016), arXiv:1604.03530 [hep-ph].
 89. C. Alexandrou, L. Leskovec, S. Meinel, J. Negele, S. Paul, M. Petschlies, A. Pochinsky, G. Rendon, and S. Syritsyn, “ $\pi\gamma \rightarrow \pi\pi$ transition and the ρ radiative decay width from lattice QCD,” *Phys. Rev.* **D98**, 074502 (2018), arXiv:1807.08357 [hep-lat].